# DELIVERY OF NEUREGULIN-1 THROUGH AN OSMOTIC TRANSPORT DEVICE (OTD)

By

Emily Wenbei Bomortino

A capstone project submitted for Graduation with University Honors

May 09, 2024

University Honors
University of California, Riverside

APPROVED

Dr. Victor Rodgers
Department of Bioengineering

Dr. Richard Cardullo, Howard H Hays Jr. Chair
University Honors

ABSTRACT

In traumatic brain injury (TBI), secondary injury involving neurological damage and edema negatively impacts recovery outcomes. Previous studies have shown that an osmotic transport device (OTD) significantly decreases severe TBI edema in rodent models. Because the OTD requires a craniectomy for direct contact to the brain, it is expected that the simultaneous delivery of the neuroprotective drug, neuregulin-1 (NRG-1), may further improve neurological outcomes. However, the release rate of NRG-1 must be controlled. In addition, because hydrogel-drug interactions can be highly complex and impact overall delivery, the release of NRG-1 from hydrogel must be analyzed. Previous research has shown that hydroxyethyl cellulose (HEC) may have the appropriate properties for this purpose. Here we test the release of the active EGF-like domain of NRG-1 from a hydrogel made up of 1.5%, 2.0%, and 2.5% HEC and artificial cerebrospinal fluid. Concentrations of the EGF domain are measured via an enzyme-linked immunosorbent assay. The results show concentration dependent Fickian diffusion behavior, with 2.0% HEC being the most promising of the hydrogels tested. Ultimately, the controlled delivery of NRG-1 integrated with an OTD will greatly improve recovery outcomes for victims of severe TBI.

ACKNOWLEDGEMENTS

Firstly, I would like to thank my wonderful faculty mentor, Dr. Victor Rodgers, who provided endless support and guidance throughout the entire process in the Biotransport and Bioreaction Kinetics (B2K) Group. Secondly, I would like to acknowledge the graduate student, Alan Giglio, who mentored me through the experiments and details of my capstone in the lab. I would also like to thank the Chancellor's Research Fellowship for supporting my researcher and giving me the opportunity to grow. Lastly, I thank University Honors for giving me this opportunity to develop and strengthen my experience in undergraduate research. I thank all the helping hands that went into making this research project a reality.

TABLE OF CONTENTS

**INTRODUCTION…….5**

**MATERIALS AND METHODS……11**

I. Concentration Model for Transient Diffusion with an Infinite Sink……...11

II. Determining Hydrogel Geometry……13

III. Determining the Effective Diffusion Coefficients of NRG-1 in HEC……14

**RESUTS AND DISCUSSION…….18**

I. Determined Hydrogel Geometry……..18

II. Effective Diffusion Coefficients of NRG-1 in HEC……20

III. Future Directions…….24

**CONCLUSION……25**

**REFERENCES…….26**

# INTRODUCTION

Annually, about 200,000 people suffer from traumatic brain injury (TBI) [1]. The initial trauma of the injury, known as primary injury, causes mechanical damage, such as broken bones, torn muscle, or damaged blood vessels. Additionally, studies show that the biological processes that come after the initial trauma, such as hemorrhage, swelling, and ischemia, cause further neurological damage. This is known as secondary injury, and it is the main contributor to the increased mortality rates in severe TBI [2]. Secondary injury is activated by the primary injury such that the physiological response causes the release of enzymes and hypoxia, which damages uninjured cells surrounding the primary injury and increasing the affected area [3]. This can lead to edema, necrosis, neurological damage, increased intracranial pressure (ICP), ischemia, oxidative stress, metabolic dysfunction, inflammation, and much more [2]. Increased ICP is of particular interest because it is a result of the brain being compressed against the skull. The ICP can increase so much that it results in the collapse of the brain stem, drastically increasing fatality of severe TBI [2,3]. Even without brain stem collapse, secondary injury can lead to long-term issues if left untreated, such as seizures, demyelination, and decreased neurogenesis [3]. Therefore, it is imperative to treat secondary injury in a timely manner to avoid the negative effects of chronic injury. Fortunately, secondary injury is reversible, meaning the long-term effects can be minimized given it is treated adequately. Secondary injury also has a relatively slow progression, allowing medical personnel enough time to treat the victim [3].

Current treatments for secondary injury involve decompressive craniectomy, hypertonic saline, and mild hypothermia. Decompressive craniectomy involves removing part of the skull to allow the brain tissue to expand outside of the head so that it is not compressed against the skull, which may reduce ICP. However, this may also result in herniated tissue, leading to cell damage

and complications [4]. Hypertonic saline also works to reduce ICP by drawing water away from the cellular environment via osmotic pressure, but the results for this therapy are mixed as some cases report complications associated with using this therapy. The most common complication seen has been the development of central pontine myelinolysis, which is the rapid shrinking of the brain and results in demyelination [4]. Mild hypothermia has been shown to be anti-inflammatory and neuroprotective, but the results are inconsistent as well [4]. These shortcomings show that consistent and efficient treatment for secondary injury in severe TBI is needed. Thus, there needs to be a therapy that consistently and efficiently treats secondary injury and improves recovery outcomes for victims of severe TBI.

One advancement in treating secondary injury is the development of an osmotic transport device (OTD), which decreases edema in rodent TBI models [5]. The device has a high concentration of bovine serum albumin (BSA) solution within it, which is separated from the water by a semipermeable membrane. BSA is a large protein that cannot pass through the pores of the membrane, however water can since it is a small molecule. This creates an external osmotic pressure gradient, which drives fluid from the site of injury and into the device. The OTD has been shown to decrease water content in edema and improve neurological functions for severe TBI in rat models [5]. Because the OTD requires a craniectomy for direct contact to the brain, it is expected that the simultaneous local delivery of a neuroprotective drug may further improve neurological outcomes. This revision to the OTD will treat edema and neurological damage simultaneously, increasing recovery outcomes for severe TBI victims. This is the focus of my work.

There are several drugs that can treat neurological damage for severe TBI, one of which is called neuregulin-1 (NRG-1). It is a neuroprotective growth factor that consists of a

transmembrane domain, epidermal growth factor (EGF)-like domain, immunoglobulin-like domain or cysteine-rich domain, and a cytoplasmic tail [6]. NRG-1 binds to the ErbB3 and ErbB4 receptors on neurons, which then affects their corresponding pathways. Experimental studies show that in severe TBI, NRG-1 increases neuronal survival, maintains the blood-brain barrier integrity, and increases functional recovery [7-10]. Additionally, introducing exogenous NRG-1 to the site of injury promotes endogenous NRG-1 expression, which reduces the dose of NRG-1 required to affect the site of injury and lowers the cost of treatment [11]. Because of these characteristics, NRG-1 is a promising drug that could further improve recovery outcomes of severe TBI.

With this background information in mind, my research investigates an OTD design that simultaneously treats edema and neurological damage, thus further improving recovery outcomes for severe TBI victims. To do this, I integrate a drug delivery system into the OTD such that NRG-1 can be delivered to the site of injury during edema removal. Specifically, I am using the active EGF-like domain of NRG-1 due to its role in activating the ErbB3 and ErbB4 pathways and its high diffusivity (i.e., small molecular weight). The drug delivery system I use is hydrogel, a network of cross-linked hydrophilic polymers that make a porous material, which allows for drug delivery [12].

One characteristic of hydrogels that make them appealing for biomedical application is that they allow for the controlled release of drugs, temporal and/or spatial. This is an important consideration in any drug delivery system since an insufficient dosage may not adequately affect the patient while excessive dosage may lead to adverse effects and/or increase cost of the treatment [13]. Additionally, most hydrogels are biocompatible, meaning they can safely be in contact with the brain [14]. Another major benefit of using hydrogel is that hydrogel is already

utilized in the OTD design for continuous brain contact [5]. Changing the type of hydrogel should not hamper the function of the OTD and will not require major modifications to the manufacturing process.

There are many properties that affect the release of solutes from a hydrogel matrix, such as the properties of the polymer itself. Surface properties, such as hydrophilicity, chemical reactivity, surface viscosity, and topography, govern the hydrogel's interactions with tissues and other biological components. Bulk properties, such as molecular weight, solubility, pore size, and mechanical stability, determine the hydrogel's release mechanism [15-17]. There are many documented release mechanisms, but for brevity, the release mechanism I am interested in is known as interior diffusion or diffusion controlled. This mechanism is applicable to non-degradable hydrogels in which drug release is purely governed by diffusion [18]. A common property used to control the release rate for this mechanism, and the one I am investigating in this research, is the percent concentration of the polymer since it is easily manipulated. Typically, the greater the polymer concentration, the slower the release of drugs from the hydrogel. This is due to a higher crosslink density, which decreases the number and size of the pores. This restricts the movements of solutes, therefore decreasing their release rate [18]. Specifically, I am researching monolithic or matrix devices, in which the solute is evenly distributed within the hydrogel matrix [16]. This simplifies the model of drug release to 1-D Fickian diffusion.

Diffusion is defined as the overall movement of molecules due to the random collisions between molecules [18]. A commonly used model to describe diffusion, and the one used in this capstone, is known as Fickian diffusion. Fickian diffusion is governed only by the concentration gradient of the solute and the diffusion coefficient of the solute in a specific solvent. Given that

the release of NRG-1 is transient in one dimension, the specific equation of interest is Fick's second law,

$$\frac{\partial C}{\partial t} = D_{ij} \frac{\partial^2 C}{\partial x^2} \quad (1)$$

where t is time, C is concentration, x is the position, and $D_{ij}$ is the diffusion coefficient. This equation states that the concentration of the diffusing species is a function of both time and space. This differential equation can be solved for concentration, C. Fick's second law assumes that no convection, mass transfer via fluidic movement, is present and the diffusion coefficient, $D_{ij}$, is independent of concentration [18]. The diffusion coefficient is of specific interest because it is a major parameter that controls the rate of diffusion. For porous media (e.g., hydrogels), the diffusion coefficient is known as the effective diffusion coefficient, $D_{eff}$, since the media is not completely fluid [18]. For NRG-1 in hydrogel, the effective diffusion coefficient is unknown, however it can be experimentally determined using the appropriate mathematical model.

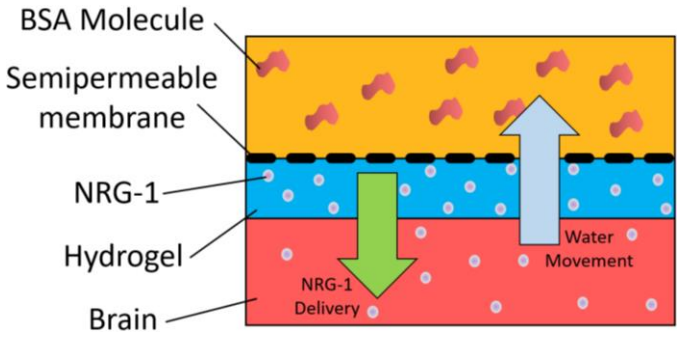


Figure 1 – The desired transport directions of NRG-1 (green arrow) into the brain and water removal (light blue arrow) from the brain during OTD operation. The goal of this work is to determine the transport characteristics of the NRG-1 in our selected hydrogel, hydroxyethyl cellulose.

While the assumption that convection is not present is true for some situations, it is not true in the case of an operating OTD. Fluid is drawn up from the body into the device while NRG-1 is simultaneously delivered to the brain, as shown in the figure above. This introduces a

convective component in the hydrogel and alters the release rate of NRG-1. This then changes Equation 1 into

$$\frac{\partial C}{\partial t} + v\frac{\partial C}{\partial x} = D_{ij}\frac{\partial^2 C}{\partial x^2} \quad (2)$$

This assumes that the fluid velocity, v, is also one dimensional and no reaction takes place [18]. This model, however, is complicated to solve analytically. Therefore, a different model known as the Peclet number is used to estimate the rate of water removal required to allow for sufficient NRG-1 delivery to the site of injury. The Peclet number (*Pe*) is a ratio of convective and diffusive forces that act on NRG-1 [18].

$$Pe = \frac{vL}{D_{eff}} \quad (3)$$

In Equation 3, $v$ is the fluid velocity, $L$ is the characteristic length, and $D_{eff}$ is the effective diffusion coefficient. The Peclet number is useful when determining whether convection or diffusion dominates species movement. If the Peclet number is much greater than one, then convection dominates and if it is much less than one, then diffusion dominates. For my application, the Peclet number should be much less than one, which indicates that diffusion dominates NRG-1 movement. This would result in NRG-1 being delivered into the brain rather than being transported into the device via convection due to water removal, which would render the drug ineffective. To determine *Pe*, the effective diffusion coefficient of NRG-1 in hydrogel must be known. However, hydrogel interactions with proteins can be complex, so the effective diffusion coefficient must be determined empirically. My research aims to determine the effective diffusion coefficient of NRG-1 in varying concentrations of HEC.

# MATERIALS AND METHODS

## I. Concentration Model for Transient Diffusion with an Infinite Sink

A mathematical model is required to determine the effective diffusion coefficient of NRG-1 in HEC. As stated in the Introduction, I will use Fick's second law (Equation 1), which can be solved for concentration using the following boundary conditions in cylindrical coordinates:

$$t \leq 0, 0 \leq z \leq h, C = C_0$$

$$t > 0, z = 0, \frac{\partial C}{\partial z} = 0$$

$$t \geq 0, z = h, C = 0$$

where *t* is time, *z* is vertical position in the hydrogel, *h* is the height of the hydrogel, and $C_0$ is the initial hydrogel concentration. The initial condition ($t \leq 0$) states the initial concentration within the hydrogel. The first boundary condition at $z = 0$ states NRG-1 does not permeate through the bottom of the hydrogel. The second boundary condition at $z = h$ as is an infinite sink approximation and assumes that, at the hydrogel surface, the concentration of NRG-1 is approximately zero. This introduces a concentration gradient which causes NRG-1 to diffuse towards the hydrogel surface. Expressing Fick's second law and the boundary conditions in dimensionless parameters allows one to scale the model to any system with the same assumptions and compare the model to other systems that may or may not have the same conditions or initial values quantitatively. We can do this using dimensionless parameters. For this study, the dimensionless parameters can be defined as such:

$$\eta = \frac{z}{h} \qquad \theta = \frac{C}{C_0} \qquad \tau = \frac{D_{ij}t}{h^2}$$

where $\eta$ is dimensionless height, $\theta$ is dimensionless concentration, and $\tau$ is the characteristic time. Plugging these dimensionless parameters into Equation 1 results in

$$\frac{\partial \theta}{\partial \tau} = D_{eff} \frac{\partial^2 \theta}{\partial \eta^2}. \tag{4}$$

The dimensionless parameters can also be input into the boundary conditions as shown below.

$$\tau \leq 0, 0 \leq \eta \leq 1, \theta = 1$$

$$\tau \geq 0, \eta = 0, \frac{\partial \theta}{\partial \eta} = 0$$

$$\tau \geq 0, \eta = 1, \theta = 0$$

These boundary conditions can be used to solve for dimensionless concentration in Equation 4 to obtain

$$\theta = \sum_{n=0}^{\infty} \frac{4\,cos(\pi n) cos\left(\left(n+\frac{1}{2}\right)\pi\eta\right)}{2n\pi+\pi} e^{-\left(\left(n+\frac{1}{2}\right)\pi\right)^2 \tau}. \tag{5}$$

For the purposes of this experiment, it is more useful to measure the accumulated mass, $M_t$, released from the hydrogel rather than the concentration. Thus, the accumulated mass model with dimensions is shown below, where *A* is the area of the hydrogel surface.

$$M_t = -AD_{eff}C_0 \sum_{n=0}^{\infty} \frac{4\pi h cos(\pi n) sin\left(\left(n+\frac{1}{2}\right)\pi\frac{z}{h}\right)}{(2n\pi+\pi)\left(n+\frac{1}{2}\right)\pi^2 D_{eff}} \left(e^{-\left(\left(n+\frac{1}{2}\right)\pi\right)^2 \frac{D_{eff}t}{h^2}} - 1\right) \tag{6}$$

This model is used to determine the effective diffusion coefficient of NRG-1 in hydrogel, $D_{eff}$ which is determined at $z = h$.

It should be noted that Equation 6 is equivalent to the model derived for a semi-infinite medium:

$$M_t = 2A\sqrt{\frac{D_{eff}t}{\pi}}(C_0 - C_1) \quad (7)$$

where $M_t$ is the amount of drug released and $C_1$ is the initial medium NRG-1 concentration. This is due to NRG-1 diffusion being limited by the hydrogel in both models, resulting in identical effective diffusion coefficients.

## II. Determining Hydrogel Geometry

Another important property that determines the release rate of drugs is the shape of the hydrogel [17]. Previous research that investigated NRG-1 diffusion in hydrogel utilized a cone-shaped tube to house the hydrogel [19]. However, an assumption of Equation 6 is that the cross-sectional area of the hydrogel is constant, which is not the case for a cone. It is difficult to determine analytically if other common tube shapes (e.g., conical, hemispherical) would yield the same result. Therefore, a simulation software that uses numerical methods, COMSOL Multiphysics [20], was compared to the results of the infinite sink transient diffusion model above, which was graphed in MATLAB. To make accurate comparisons, the volume of the hydrogel remained the same (0.5 mL) across all models and the heights and areas were corrected for each shape. The geometry of the models is shown in the figure below. The parameters, kept constant for all three geometries, were $1 \times 10^{-7}$ $cm^2/s$ for the effective diffusion coefficient ($D_{eff}$), 20 ng for the initial mass ($M_0$), and 40 ng/mL for the initial concentration ($C_0$). The physics module used was the transient transport of diluted species module and mesh independence was achieved. For the COMSOL model, the flux was evaluated every thirty minutes for a total time of three hours to mimic the experimental procedure in the next section. The fractional accumulated mass was compared between Equation 6 and the COMSOL models for each

geometry to determine if hydrogel geometry affects the effective diffusion coefficient of NRG-1 in HEC.

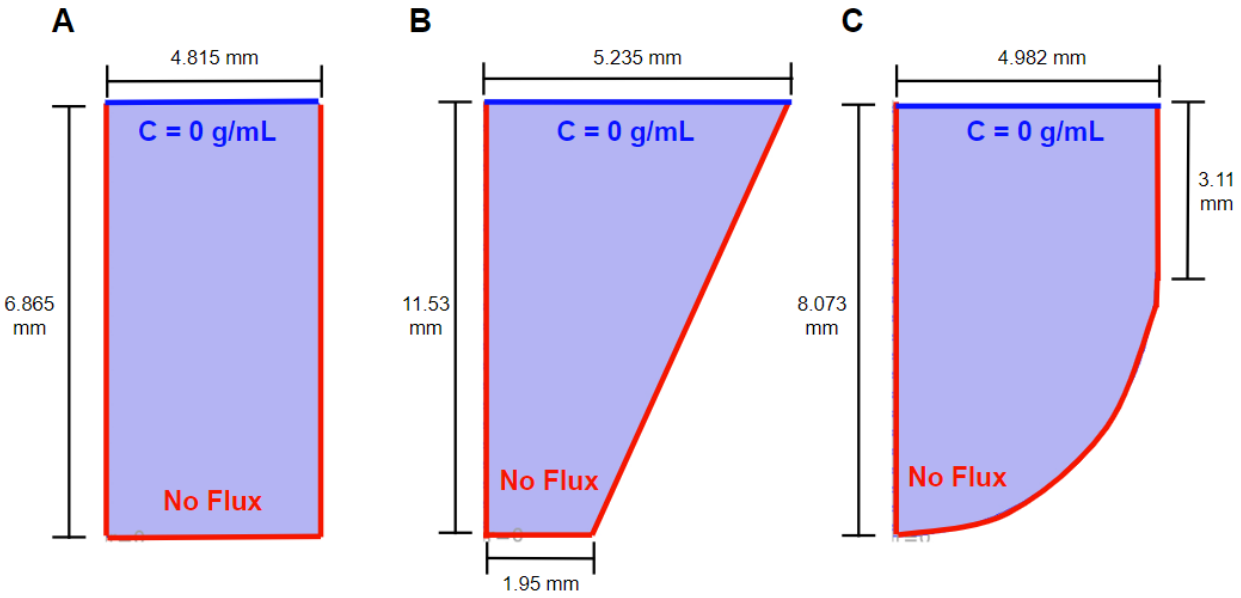


Figure 2 – The dimensions and boundary conditions for the cylindrical, conical, and hemispherical COMSOL models, respectively. The red lines signify a Neumann condition in which the flux is zero. The blue lines show a Dirichlet condition in which the concentration is 0 g/mL.

## III. Determining the Effective Diffusion Coefficients of NRG-1 in HEC

Figure 3 below depicts the experimental setup in an orbital shaker. The hydrogel used for this experiment was hydroxyethyl cellulose (HEC) due to its biocompatibility, availability, solubility in artificial cerebrospinal fluid (aCSF), cost, and ease of preparation [21,22]. Additionally, HEC does not require heat to crosslink, unlike alginate which was used in the OTD in previous studies [5]. High temperatures can denature NRG-1, rendering it ineffective. The HEC hydrogel percent concentrations observed were 1.5%, 2.0%, and 2.5% by mass percent. The hydrogel was loaded with 1 µg/mL of carrier free EGF-like domain of NRG-1 (396-HB-050/CF, R&D Systems) during gelation with aCSF as the solvent for a final volume of 1 mL. Once gelation was complete, 0.5 mL of the NRG-1 loaded hydrogel was transferred to a cylindrical tube (see

Results I) and the hydrogel diameter and height was measured to utilize in Equation 6. Once the hydrogel dimensions were measured, 1 mL of aCSF was placed on top to introduce a concentration gradient while maintaining electrochemical equilibrium. Electrochemical equilibrium ensures that the release of NRG-1 from the hydrogel is solely due to NRG-1 diffusion and not ion movement. Ion movement could increase the release of NRG-1 from the hydrogel, leading to an inaccurate effective diffusion coefficient. The tube was then placed in an orbital shaker at 50 rpm to minimize the effects of a boundary layer over the hydrogel [23,24]. I want to minimize the boundary layer because it may decrease the NRG-1 release rate from the hydrogel and lead to an inaccurate effective diffusion coefficient. For three hours, every thirty minutes, the aCSF was removed and replaced with fresh aCSF to satisfy the infinite sink boundary condition. The removed aCSF was used to determine the amount of NRG-1 released over time via an enzyme-linked immunosorbent assay (ELISA).

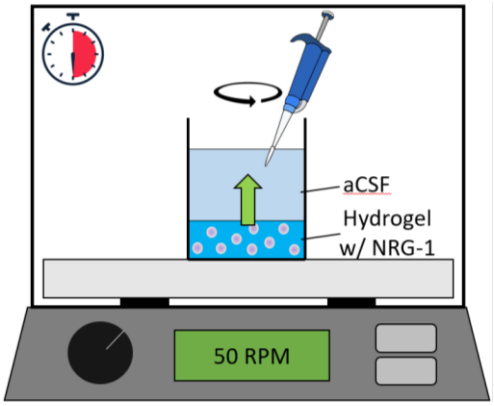


Figure 3 - The experimental setup to determine the effective diffusion coefficient of NRG-1 in various HEC hydrogel percent concentrations. The hydrogel is placed in the orbital shaker at 50 rpm and the aCSF above it is replenished every thirty minutes for three hours.

An ELISA works by using antibodies to detect the analyte, in my case the EGF-like domain of NRG-1. There is a capture antibody, which binds to the plate and captures the analyte when it is introduced. However, this by itself cannot determine the concentration of NRG-1. Therefore, a

detection antibody is used to help determine the concentration of the analyte through colorimetric means. Detection antibodies are normally conjugated with biotin so that a reporter enzyme, usually streptavidin horseradish peroxidase (HRP), can bind to the detection antibody. The enzyme converts a substrate to a product which has a readable color. After a certain amount of time, a stop solution is introduced to ensure the reaction does not saturate the solution with color. This process is depicted in Figure 4 below for a successful binding event.

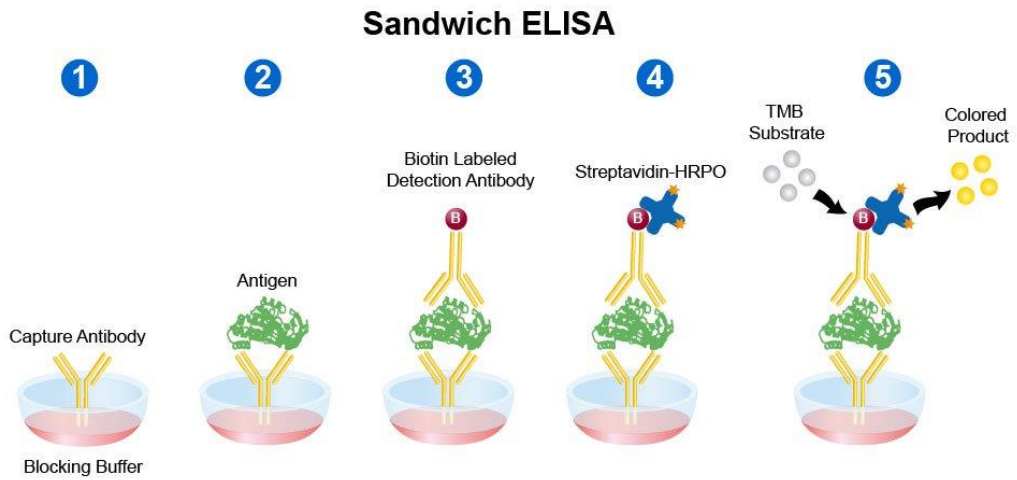


Figure 4 – A sandwich ELISA using a capture antibody, a biotin labeled detection antibody, streptavidin-HRP, and TMB substrate to acquire a reading. The antigen binds to the capture antibody, which allows the detection antibody to bind to the antigen. This then allows the streptavidin-HRP to bind to the biotin, which allows the enzyme to produce a signal by acting on the TMB substrate. Image from [25].

Initially, the ELISA antibodies for the NRG-1-β1 domain (DY377, R&D Systems) were used to determine the concentrations of NRG-1 released over time. However, since those antibodies were manufactured to detect the entire NRG-1- β1 domain, they had low sensitivity to the EGF-like domain of NRG-1. Because of this, different antibodies were used and optimized to detect the EGF-like domain of NRG-1 at low concentrations. Human NRG-1 EGF domain antibody (AF-396-SP, R&D Systems) was used as the capture antibody and human NRG-1- β1 extracellular domain biotinylated antibody (BAF377, R&D Systems) was used as the detection antibody. Streptavidin-HRP was the enzyme used to allow color development,

tetramethylbenzidine (TMB) was the substrate, and sulfuric acid was the stop solution. The ELISA plate was blocked with 1% BSA for 1 hour and washed 4 four times for each reagent necessary. A nonlinear regression model using MATLAB [26] for Equation 6 was used to determine the effective diffusion coefficients for each hydrogel.

# RESULTS & DISCUSSION

## I. Determined Hydrogel Geometry

The results of implementing the corresponding surface radii and hydrogel heights into Equation 6 are shown in the release behavior graphed below. The fractional accumulated mass between the three geometries begins to diverge as time increases, indicating that the derived model cannot account for all three geometries.

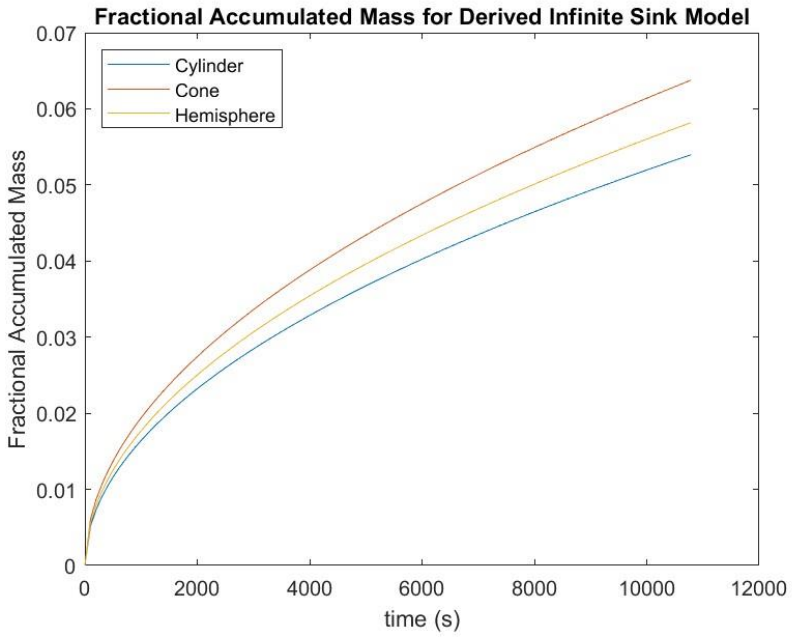


Figure 5 - The graphical representation of the derived infinite sink model for fractional accumulated mass over three hours for cylindrical (blue), conical (red), and hemispherical (yellow) hydrogel geometries. The release behavior begins to diverge as time increases.

To verify that the derived model and the COMSOL model were comparable, the fractional accumulated mass behavior for the cylindrical COMSOL model was graphed against the cylindrical derived model since Equation 6 assumes a geometry in which the cross-sectional area is constant (i.e., a cylinder). Similar behaviors indicate that the models were indeed comparable.

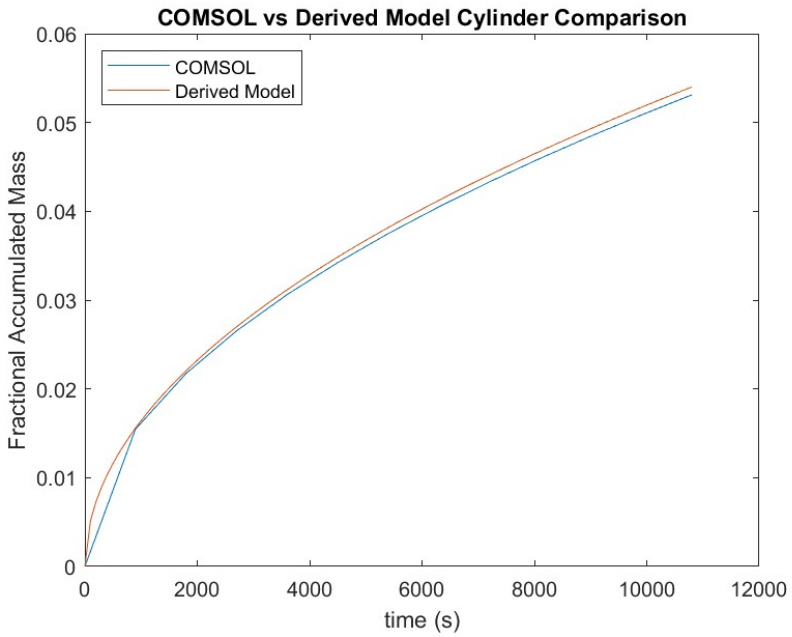


Figure 6 - The fractional accumulated mass of the cylindrical geometries of the derived model (orange) and the COMSOL (blue) model. They exhibit extremely similar behaviors.

The release behaviors of the conical and hemispherical geometries are shown in Figure 7 below. The difference between the infinite sink derived models and the COMSOL models indicates that Equation 6 cannot account for other hydrogel geometries. The conical geometry results in a difference of $3 \times 10^{-8}$ $cm^2/s$ and the hemispherical geometry results in a difference of $1.3 \times 10^{-8}$ $cm^2/s$ for the assumed effective diffusion coefficient of $1 \times 10^{-7}$ $cm^2/s$. Therefore, a cylindrical tube must be used to calculate an accurate effective diffusion coefficient with Equation 6.

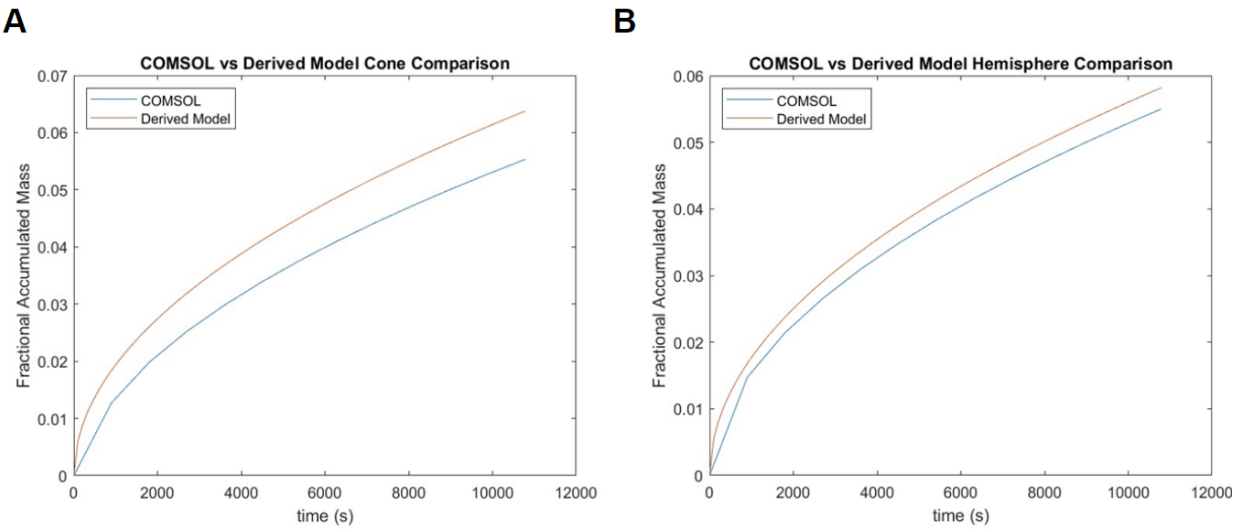


Figure 7 - The fractional accumulated mass of the conical (A) and hemispherical (B) geometries of the derived model (orange) and the COMSOL model (blue). There is a $3 \times 10^{-8}$ $cm^2/s$ difference between the conical models and a $1.3 \times 10^{-8}$ $cm^2/s$ difference between the hemispherical models for an assumed effective diffusion of $1 \times 10^{-7}$ $cm^2/s$.

## II. Effective Diffusion Coefficients of NRG-1 in HEC

Using the optimized ELISA antibodies, the results from the experiment are shown below. In Figure 8, the standard curve with a logarithmic fit is shown. This standard curve is used to translate optical density (OD) measurements to concentration in ng/mL, specifically the equation for the curve of best fit. After utilizing the standard curve, the results of the release study are shown in Figure 9. The 2.5% HEC hydrogel has the slowest release rate as shown by the relatively low NRG-1 concentrations after three hours. The 1.5% hydrogel has the next fastest release rate, and the 2.0% hydrogel has the fastest release rate since it released the most NRG-1.

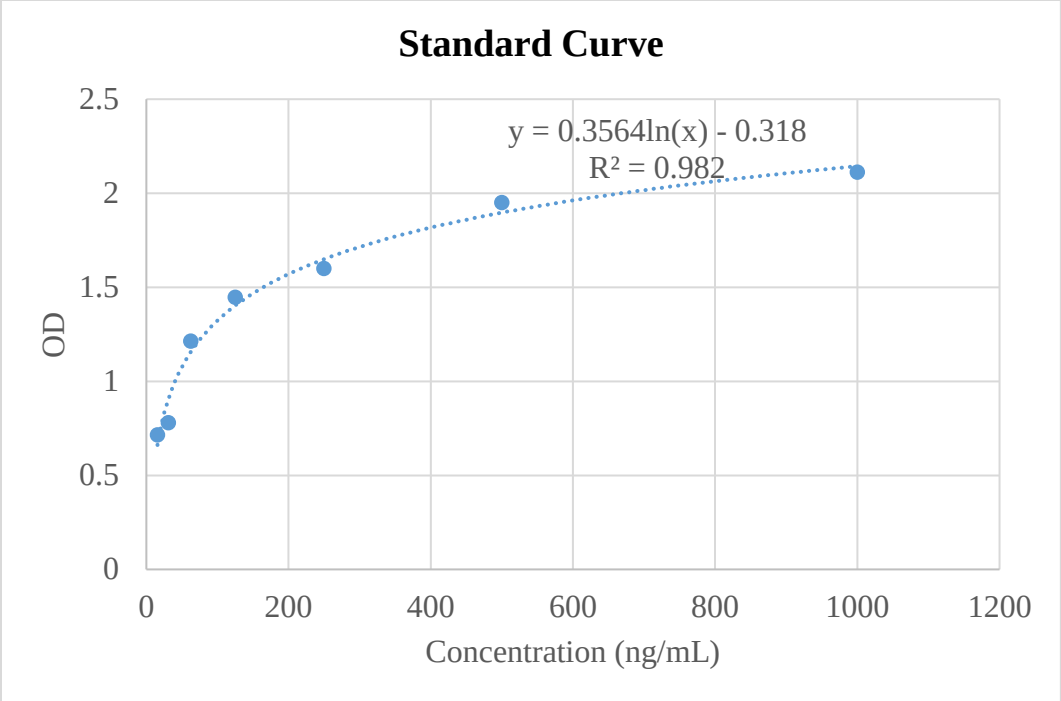


Figure 8 – The standard curve used to determine concentration from OD. The points are samples of known concentration plotted against their measured OD values. The dotted line is the curve of best fit, a logarithmic function, that was used to determine concentration in ng/mL from OD. The $R^2$ value was 0.982.

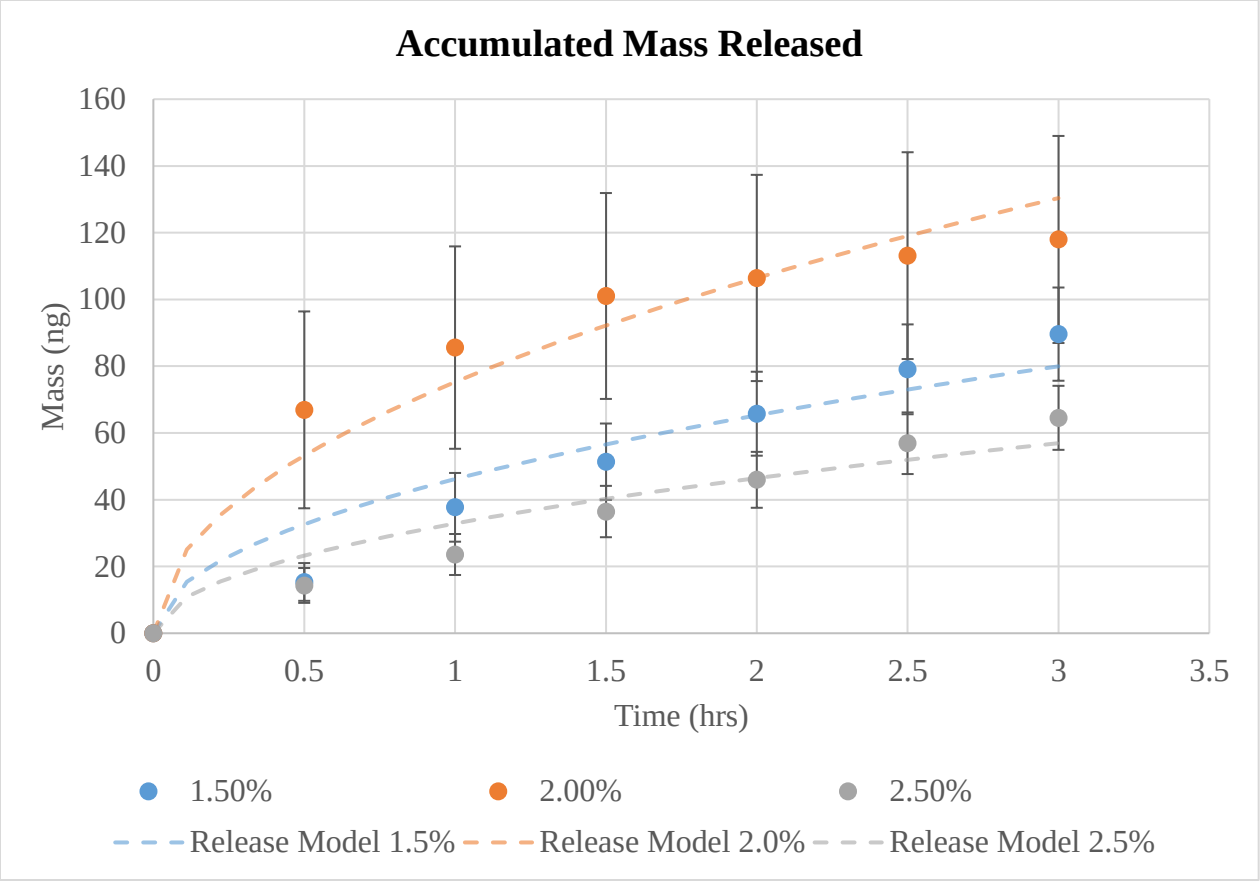


Figure 9 - The accumulated mass of NRG-1 released over three hours. The points represent concentrations determined by the ELISA and the dashed line represents the nonlinear regression fit for equation 6. The 2.5% HEC hydrogel (gray) released the slowest, the 1.5% HEC hydrogel (blue) released faster, and the 2.0% HEC hydrogel (orange) released the fastest of all three hydrogels.

The height and diameter of the hydrogels were measured and, along with the results above, input into the nonlinear regression model for Equation 6 in MATLAB, giving the effective diffusion coefficients for each HEC concentration. The 1.5% HEC hydrogel had an effective diffusion coefficient of $(1.708 \pm 0.213) \times 10^{-7}$ cm$^2$/s, the 2.0% HEC hydrogel had an effective diffusion coefficient of $(4.540 \pm 0.360) \times 10^{-7}$ cm$^2$/s, and the 2.5% HEC hydrogel had an effective diffusion coefficient of $(0.866 \pm 0.108) \times 10^{-7}$ cm$^2$/s. The result for the 2.5% HEC makes sense given that it is the most densely cross-linked hydrogel and therefore, has the slowest NRG-1 release rate. The effective diffusion coefficients for the 1.5% and 2.0% HEC are more of a surprise since it was originally expected that the 1.5% HEC would have the fastest release rate

given it has the lowest cross-linked density. However, these results do not reflect this expectation. Given the complexity of hydrogel-drug interactions, more studies must be done to determine the reason why the 2.0% HEC released NRG-1 the fastest rather than the 1.5% HEC.

However, these results can be compared to other known diffusion coefficients of other proteins to ensure the results are reasonable. The characteristic considered is the size of the protein given that molecular weight affects the diffusion coefficient [18]. Insulin with a molecular weight of 6 kDa and BSA with a molecular weight of 66 kDa are considered because they are below and above the size of NRG-1 (8 kDa), respectively. The diffusion coefficient of insulin is $15 \times 10^{-7}$ $cm^2/s$ [27] while the diffusion coefficient of BSA is $6.1 \times 10^{-7}$ $cm^2/s$ [18] in water. It must be noted that these diffusion coefficients are for these proteins in water, meaning they are higher than they would be in hydrogel. However, they are still the same order of magnitude as the effective diffusion coefficients for NRG-1 in HEC, implying the results are reasonable.

Secondly, the diffusive flux must be considered in the context of an operating OTD. Remember that water is removed from the brain and into the device while NRG-1 is being delivered into the brain. This implies the Peclet number needs to be much less than one, meaning the effective diffusion coefficient must be much larger than the numerator to satisfy this condition. Of the three hydrogels observed, the 2.0% hydrogel has the largest effective diffusion coefficient. This implies an HEC concentration of 2.0% is the most promising hydrogel to integrate into the OTD.

## III. Future Directions

While these results are promising, it would be beneficial to verify these results with more trials to ensure the effective diffusion coefficients calculated are correct for each hydrogel. Additionally, the water removal rate that allows for sufficient NRG-1 diffusion into the brain can be estimated with the Peclet number, however more concrete results will have to be determined. BSA concentration should be investigated due to its effect on water removal rate for the OTD. Another direction that can be investigated from this project is the semipermeable membrane. Currently, the semipermeable membrane does not allow BSA to pass, however its pores are large enough that NRG-1 can pass through. This may decrease the efficacy of NRG-1 even if optimal convection conditions are satisfied. Therefore, decreasing the membrane pore size such that neither BSA nor NRG-1 can pass through, but water can, may be beneficial to increasing drug delivery. Lastly, researching other biocompatible hydrogels and their NRG-1 release rates may provide additional options for the type of hydrogel that will ultimately be integrated into the OTD to allow for simultaneous NRG-1 delivery and fluid removal.

# CONCLUSION

The simulated results from COMSOL Multiphysics show that geometry is an important consideration when experimentally determining diffusion coefficients. It was determined that using cylindrical geometry allows for more accurate results for the mathematical model used. Compared to the cylindrical geometry, the conical geometry deviated $3 \times 10^{-8}$ $cm^2/s$ and the hemispherical geometry resulted in a difference of $1.3 \times 10^{-8}$ $cm^2/s$ for an assumed diffusion coefficient of $1 \times 10^{-7}$ $cm^2/s$. Considering these results, a cylindrical tube was used to determine the effective coefficients of NRG-1 in varying concentrations of HEC. The results show that the 2.0% HEC hydrogel with a diffusion coefficient of $(4.540 \pm 0.360) \times 10^{-7}$ $cm^2/s$ has the most potential to sufficiently deliver NRG-1 to the site of injury. Further experiments will be needed to verify the results above as well as characterize how water removal via the OTD affects NRG-1 delivery. Additionally, other hydrogels and their NRG-1 effective diffusion coefficients can be studied and compared to these results. The pore size of the semipermeable membrane may also be altered for future studies.

REFERENCES


[1] Peterson, Alexis B., et al. “Surveillance Report of Traumatic Brain Injury-related Deaths by Age Group, Sex, and Mechanism of Injury,” *Centers for Disease Control and Prevention*, 2022.

[2] Merrick, Mark A. “Secondary Injury After Musculoskeletal Trauma: A Review and Update.” *Journal of Athletic Training*, vol. 37, no. 2, pp. 209–217, Apr-June 2002.

[3] Kaur, Parmeet and Saurabh Sharma. “Recent Advances in Pathophysiology of Traumatic Brain Injury.” *Current Neuropharmacology*, vol. 16, no. 8, pp. 1224–1238, Oct. 2018.

[4] Bayir, Hülya, Robert S. B. Clark, and Patrick M. Kochanek. “Promising strategies to minimize secondary brain injury after head trauma.” *Critical Care Medicine*, vol. 31, no. 1, pp. 112–117, Jan. 2023, doi:10.1097/00003246-200301001-00016.

[5] McBride DW, Szu JI, Hale C, Hsu MS, Rodgers VGJ, Binder DK (2014) Reduction of Cerebral Edema After TBI using an Osmotic Transport Device, Journal of Neurotrauma, 31:1948–1954, doi:10.1089/neu.2014.3439.

[6] Falls, D.L., “Neuregulins: functions, forms, and signaling strategies.” *Experimental Cell Research*, vol. 284, no. 1, pp. 14–30, 2003.

[7] Navarro-González, Carmen, et al, “NRG1 Intracellular Signaling Is Neuroprotective upon Stroke,” *Oxidative Medicine and Cellular Longevity*, vol. 2019, pp. 1–15, 8 Sept. 2019, doi:10.1155/2019/3930186.

[8] Yan, Feng, et al, “Erbb4 Protects against Neuronal Apoptosis via Activation of Yap/PIK3CB Signaling Pathway in a Rat Model of Subarachnoid Hemorrhage,” *Experimental Neurology*, vol. 297, pp. 92–100, 17 July 2017, doi:10.1016/j.expneurol.2017.07.014.

[9] Qian, Huan, et al. “Erbb4 Preserves Blood-Brain Barrier Integrity via the Yap/PIK3CB Pathway after Subarachnoid Hemorrhage in Rats.” *Frontiers in Neuroscience*, vol. 12, 24 July 2018, doi:10.3389/fnins.2018.00492.

[10] Iaci, Jennifer F., et al. “An Optimized Dosing Regimen of CIMAGLERMIN (Neuregulin 1β3, Glial Growth Factor 2) Enhances Molecular Markers of Neuroplasticity and Functional Recovery after Permanent Ischemic Stroke in Rats.” *Journal of Neuroscience Research*, vol. 94, no. 3, pp. 253–265, 11 Mar. 2015, doi:10.1002/jnr.23699.

[11] Peterson, Allison R., et al. “Regulation of NRG-1-ErbB4 signaling and neuroprotection by exogenous neuregulin-1 in a mouse model of epilepsy.” *Neurobiology of Disease*, vol. 161, Dec. 2021, doi:.1016/j.nbd.2021.105545.

[12] Temenoff, Johnna S. and Antonios G. Mikos. *Biomaterials: The Intersection of Biology and Materials Science.* Upper Saddle River, New Jersey: Pearson Prentice Hall Bioengineering, 2008.

[13] Fricker, Florence R, and David LH Bennett. “The role of neuregulin-1 in the response to nerve injury.” *Future Neurology*, vol. 6, no. 6, Nov. 2011, pp. 809–822, doi:10.2217/fnl.11.45.

[14] Hoffman, Allan S. “Hydrogels for Biomedical Applications.” *Annals of the New York Academy of Sciences*, vol. 944, no. 1, pp. 62–73, 2001, doi:10.1111/j.1749-6632.2001.tb03823.x.

[15] Vashist, Arti and Sharif Ahmad. “Hydrogels: Smart Materials for Drug Delivery.” *Oriental Journal of Chemistry*, vol. 29, no. 3, pp. 861–870, 4 Aug. 2014, doi:10.13005/ojc/290303.

[16] Omathanu, Pillai and Ramesh Panchagnula. “Polymers in Drug Delivery.” *Current Opinion in Chemical Biology,* vol. 5, no. 4, pp. 447–451, 1 Aug. 2001, doi:10.1016/S1367-5931(00)00227-1.
[17] Zarzycki, Roman, Zofia Modrezejewska, and Katarzyna Nawrotek. “Drug Release from Hydrogel Matrices.” *Ecological Chemistry and Engineering S*, vol. 17, no. 2, 1 Jan. 2010.
[18] Truskey, George A., Fan Yuan, and David F. Katz. *Transport Phenomena in Biological Systems.* 2nd ed. Upper Saddle River, New Jersey: Pearson Prentice Hall, 2009.
[19] Jennifer S. Yang. “Scale up of Osmotic Transport Device (OTD) to Reduce Edema and Deliver Drugs in Severe Traumatic Brain Injury: Application with Neuregulin-1.” 24 Feb. 2021.
[20] COMSOL Multiphysics® v. 6.2. www.comsol.com. COMSOL AB, Stockholm, Sweden.
[21] Sannino, Alessandro, Christian Demitri, and Marta Madaghiele. “Biodegradable Cellulose based Hydrogels: Design and Applications.” *Materials*, vol. 2, no. 2, pp. 353–373, 16 Apr. 2009, doi:10.3390/ma2020353.
[22] Vlaia, Lavinia, et al. “Cellulose-Derivatives-Based Hydrogels as Vehicles for Dermal and Transdermal Drug Delivery.” *Emerging Concepts in Analysis and Applications of Hydrogels*, pp. 159–200, 24 Aug. 2016, doi:10.5772/63953.
[23] Peppas, Nikolaos A. “Poly(ethylene glycol)-containing hydrogels in drug delivery.” *Journal of Controlled Release*, vol. 62, no. 1, pp. 81–87, 1 Nov. 1999, doi: 10.1016/S0168-3659(99)00027-9.
[24] Falk, B., S. Garramone, and S. Shivkumar. “Diffusion coefficient of paracetamol in a chitosan hydrogel.” *Materials Letters*, vol. 58, no. 28, pp. 3261–3265, 1 Oct. 2004, doi: 10.1016/j.matlet.2004.05.072.
[25] “Sandwich ELISA Protocol.” *Lenico Technologies.*
[26] The MathWorks, Inc. (2022). *MATLAB version: 9.13.0 (R2022b)*: https://www.mathworks.com.
[27] Vogel, S., *Life's Devices.* 1988, pp. 105-129, Princeton University Press, Princeton.